(the first value in parentheses) than in ethanol (the second value in parentheses). These findings indicate that the half-wave potentials in the solvents having the same functional group correspond well to the coordination powers of the solvents. The comparison of half-wave potentials measured in different solvents is accompanied by extreme difficulties. In this sense, the above facts should be noted.

Gibbs free energies of transfer of copper(II) ion from water to other solvents also correlate with the coordination power: The energies for dmf, MeOH, MeCN, EtOH, *n*-PrOH, *i*-PrOH, and pc are −11.6, −4.3, +6.2, +14.2, +11.0, +10.3, +15.9, and +17.9 kcal mol^{-1}, respectively.[44]

Conclusion

The values of the coordination power obtained in this work give a theoretically approximate representation, since the considerations of activity of a solvent and the *mer*/*fac* ratio of nickel solvate ions in the mixed solvents are ignored. Nevertheless, the coordination power successfully explains the solvent effects on the stability constants of metal complexes, the redox potentials, ligand substitutions, and d–d splitting of metal solvate ions. The coordination power series reflects well the strength of the metal ion–solvent interaction, especially for the solvents having the same functional group, and holds for hard, borderline, and soft metal ions with the except of soft bases such as MeCN. These facts strongly support that the concept of the coordination power is experimentally reliable and highly useful as a measure for the solvent donor ability, because we have no such measure except the donor number.

Acknowledgment. Thanks are given to S. Niina, T. Tateshita, T. Aboshi, T. Imai, and Y. Kushibe for their assistance in the experimental work. This work was supported in part by a Grant-in-Aid for Scientific Research from the Ministry of Education (No. 36202).

Registry No. $Ni(py)_6^{2+}$, 20037-72-3; $Ni(Me_2SO)_6^{2+}$, 26745-60-8; $Ni(H_2O)_6^{2+}$, 15365-79-4; $Ni(dmf)_6^{2+}$, 33789-00-3; $Ni(def)_6^{2+}$, 45318-23-8; $Ni(MeCN)_6^{2+}$, 15554-59-3; $Ni(PrCN)_6^{2+}$, 95725-15-8; $Ni(PhCN)_6^{2+}$, 47873-95-0; $Ni(AN)_6^{2+}$, 67486-29-7; $Ni(tmp)_6^{2+}$, 45320-88-5; $Ni(MeOH)_6^{2+}$, 18443-63-5; $Ni(EtOH)_6^{2+}$, 25286-14-0; $Ni(n\text{-}PrOH)_6^{2+}$, 42493-31-2; $Ni(n\text{-}BuOH)_6^{2+}$, 63872-29-7; $Ni(i\text{-}BuOH)_6^{2+}$, 45303-58-0; $Ni(i\text{-}PrOH)_6^{2+}$, 45283-62-3; $Ni(s\text{-}BuOH)_6^{2+}$, 63872-30-0; $Ni(t\text{-}BuOH)_6^{2+}$, 63872-31-1; $Ni(n\text{-}PeOH)_6^{2+}$, 63911-14-8; $Ni(n\text{-}HxOH)_6^{2+}$, 95725-16-9; $Ni(Me_2CO)_6^{2+}$, 25139-60-0; $Ni(pc)_6^{2+}$, 72794-87-7; py, 110-86-1; dmf, 68-12-2; def, 617-84-5; AN, 107-13-1; tmp, 512-56-1; pc, 108-32-7; bpy, 366-18-7; Me_2SO, 67-68-5; H_2O, 7732-18-5; PrCN, 107-12-0; PhCN, 100-47-0; MeCN, 75-05-8; MeOH, 67-56-1; EtOH, 64-17-5; *n*-PrOH, 71-23-8; *n*-BuOH, 71-36-3; *i*-BuOH, 78-83-1; *i*-PrOH, 67-63-0; *s*-BuOH, 78-92-2; *t*-BuOH, 75-65-0; *n*-PeOH, 71-41-0; *n*-HxOH, 111-27-3; Me_2CO, 67-64-1; Ni, 7440-02-0.

Supplementary Material Available: Listings of stability constants and half-wave potentials and a plot of the dissociation rate constant vs. coordination power (3 pages). Ordering information is given on any current masthead page.

(44) Coetzee, J. F.; Istone, W. K. *Anal. Chem.* **1980**, *52*, 53.
(45) Sone, K.; Kato, M. *Naturwissenschaften* **1958**, *45*, 10.
(46) Irving, H.; Mellor, D. H. *J. Chem. Soc.* **1962**, 5237.
(47) Canani, S.; Scrocco, E. *J. Inorg. Nucl. Chem.* **1958**, *8*, 332.

Contribution from the Department of Chemistry, Purdue University, West Lafayette, Indiana 47907, and Molecular Structure Center, Indiana University, Bloomington, Indiana 47401

Dinuclear Aryloxide Chemistry. 3.[1] Synthesis, Structure, and Fluxional Behavior of 1,2-Bis(2-*tert*-butyl-6-methylphenoxy)tetrakis(dimethylamido)dimolybdenum and -ditungsten (M≡M)

TIMOTHY W. COFFINDAFFER,[†] IAN P. ROTHWELL,*[†] and JOHN C. HUFFMANN[‡]

Received May 17, 1984

Addition of 2-*tert*-butyl-6-methylphenol (HOAr) to the dinuclear compounds $M_2(NMe_2)_6$ (M = Mo, W) results in the formation of the complexes 1,2-$M_2(OAr)_2(NMe_2)_4$ [M = Mo (**1**), W (**2**)] as yellow crystalline solids. Spectra are consistent with the presence in solution of the gauche rotamer for these complexes, and variable-temperature studies allow the activation energy for restricted rotation about the M–NMe_2 bonds to be estimated. A single-crsytal X-ray diffraction study of **1** shows that in the solid state the gauche rotamer is maintained for the unbridged $Mo_2O_2N_4$ skeleton. Crystal data at −160 °C were a = 13.532 (4) Å, b = 16.634 (6) Å, c = 14.696 (10) Å, Z = 4, and d_{calcd} = 1.369 g cm^{-3} for space group $P2_12_12_1$. The metal–metal distance of 2.2198 (14) Å is consistent with the retention of a Mo–Mo triple bond while the Mo–NMe_2 distances of 1.925–1.97 Å indicate the presence of considerable nitrogen p to metal d π bonding.

Introduction

Our discovery of the ability of some mononuclear early-transition-metal systems to activate (cyclometalate) the aliphatic bonds in the sterically bulky ligand 2,6-di-*tert*-butylphenoxide[2-4] has prompted us to investigate other situations where metalation of the alkyl side chains of aryloxide ligands may take place. In particular, we have been exploring the possibility of cyclometalation of such ligands at di-metal centers.[1] Recent results by Cotton and Walton have shown that it is possible to activate the aromatic CH bonds in the ligand 2-(diphenylphosphino)-pyridine on a Re_2^{4+} core.[5] Earlier work by Andersen and Wilkinson showed that the γ-hydrogen of alkyl ligands could also be activated across an Mo_2^{4+} core.[6] This rationale has led us to survey the reactivity of sterically demanding 2,6-dialkylphenoxides coordinated to both Mo_2^{6+} and W_2^{6+} (M≡M) cores.[1,7-9] In a number of reactions we have found reactivity both novel and complimentary compared to the previously well-documented

[†] Purdue Univesity.
[‡] Indiana University.

(1) Part 2. Coffindaffer, T. W.; Rothwell, I. P.; Huffman, J. C., *Inorg. Chem.* **1984**, *23*, 1433.
(2) Chamberlain, L.; Rothwell, I. P.; Huffmann, J. C. *Organometallics* **1982**, *1*, 1538.
(3) Chamberlain, L.; Rothwell, I. P.; Huffman, J. C. *J. Am. Chem. Soc.* **1982**, *104*, 7338.
(4) Chamberlain, L.; Rothwell, I. P. *J. Am. Chem. Soc.* **1983**, *105*, 1665.
(5) Barder, T. J.; Cotton, F. A.; Powell, G. L.; Tetrick, S. M.; Walton, R. A. *J. Am. Chem. Soc.* **1984**, *106*, 1323.
(6) Andersen, R. A.; Jones, R. A.; Wilkinson, G. *J. Chem. Soc., Dalton Trans.* **1978**, 446.
(7) Coffindaffer, T. W.; Rothwell, I. P., Huffman, J. C. *Inorg. Chem.* **1983**, *22*, 2906.
(8) Coffindaffer, T. W.; Rothwell, I. P.; Huffman, J. C. *Inorg. Chem.* **1983**, *22*, 2906.
(9) Coffindaffer, T. W.; Rothwell, I. P.; Huffman, J. C. *J. Chem. Soc., Chem. Commun.* **1983**, 1269.

0020-1669/85/1324-1643$01.50/0

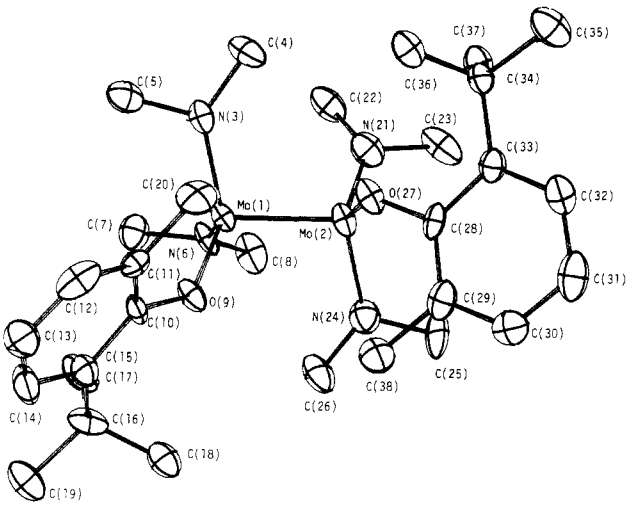

Figure 1. ORTEP view and labeling scheme for $Mo_2(OAr)_2(NMe_2)_4$ (**1**) (OAr = 2-*tert*-butyl-6-methylphenoxide).

chemistry associated with alkoxide ancillary ligands.[10,11] In this paper we describe our results obtained with the asymmetric ligand 2-*tert*-butyl-6-methylphenoxide, a ligand that offers the possibility of being metalated not only across the metal–metal bond but also to the same metal to which the oxygen is coordinated.

Results and Discussion

Two methods were used to introduce this ligand onto the M_2^{6+} center. The first involved metathetic exchange between LiOAr (OAr = 2-*tert*-butyl-6-methylphenoxide) and the compound 1,2-$Mo_2Br_2R_4$ (R = CH_2SiMe_3). This approach had been successful for the less crowded ligand 2,6-dimethylphenoxide (OAr′) and had led to both the simple substitution product 1,2-$Mo_2(OAr')_2R_4$ and an interesting alkylidyne hydride on treatment with pyridine.[9] However, the more sterically crowded LiOAr reacted much more slowly and did not give any identifiable products. Hydrocarbon solutions of LiOAr (>2 equiv) and 1,2-$Mo_2Br_2R_4$ became dark on standing at 25 °C and gave a dark brown solution after 24 h. The only identifiable product was Me_4Si. Monitoring the mixture by ^1H NMR showed the disappearance of the dibromide in C_6D_6 with the generation of large amounts of Me_4Si. Addition of ligands such as pyridine or trimethylphosphine did not allow the isolation of any stable products. This decomposition we believe is due to α-hydride abstraction occurring for the CH_2SiMe_3 groups, leading to alkylidene or alkylidyne functions, caused by the large steric bulk of the OAr ligands.[9,12] We have no evidence that activation of the CH bonds in the OAr ligand occurs during the reaction although the ultimate fate of these groups is unknown, only small amounts of HOAr being detected by ^1H NMR.

In contrast to the situation with alkyl coligands, stable complexes of OAr on both an Mo_2^{6+} and W_2^{6+} center can be readily synthesized by addition of the parent phenol HOAr (HOAr = 2-*tert*-butyl-6-methylphenol) to the hexakis(dimethylamido) complexes $M_2(NMe_2)_6$ (M = Mo,W).[13] Hence, addition of HOAr (>2 equiv) to $M_2(NMe_2)_6$ in benzene slowly forms the 1,2-disubstituted $M_2(OAr)_2(NMe_2)_4$ [M = Mo (**1**), W (**2**)]. Removal of solvent and generated dimethylamine followed by dissolution in hexane allowed the isolation of the products as pale yellow crystals. Both compounds are soluble in hydrocarbon solvents and are extremely sensitive to air in solution and the solid state, turning dark brown and finally black. Attempts to substitute NMe_2 groups further with HOAr proved fruitless. This compares with the total substitution possible with 2,6-dimethylphenol to yield the hexaaryloxide.[8] With the even more sterically demanding 2,6-di-*tert*-butylphenol, no substitution could be achieved on

Table I. Summary of the Crystallographic Data for the Compound **1**

formula	$Mo_2N_4O_2C_{30}H_{54}$
fw	694.66
space gp	$P2_12_12_1$
a, Å	13.532 (4)
b, Å	16.634 (6)
c, Å	14.969 (10)
Z	4
V, Å^3	3369.20
d(calcd), g/cm^3	1.370
cryst size, mm	0.12 × 0.12 × 0.14 mm
cryst color	pale yellow
radiation	Mo Kα (λ = 0.710 69 Å)
linear abs coeff, cm^{-1}	7.555
temp, °C	−160
detector aperture	3.0 mm wide × 4.0 mm high; 22.5 cm from cryst
sample to source dist, cm	23.5
takeoff angle, deg	2.0
scan speed, deg/min	4.0
scan width, deg	2.0 + 0.692 tan θ
bkgd counts, s	10 at each end of scan
2θ range, deg	6–45
no. of data collcd	2565
no. of unique data	2502
no. of unique data with $F_o > \sigma(F)$	2355
$R(F)$	0.046
$R_w(F)$	0.045
goodness of fit	1.191
largest Δ/σ	0.05

Table II. Fractional Coordinates and Isotropic Thermal Parameters for Compound **1**

atom	10^4x	10^4y	10^4z	B_{iso}, Å^2
Mo(1)	−59 (1)	966 (1)	8590 (1)	21
Mo(2)	789 (1)	9285 (1)	9787 (1)	18
N(3)	705 (9)	10568 (6)	8157 (6)	33
C(4)	1606 (12)	10956 (8)	8420 (9)	35
C(5)	253 (13)	11039 (8)	7423 (10)	37
N(6)	8688 (8)	25 (6)	9107 (7)	30
C(7)	−2021 (11)	10281 (9)	8487 (10)	43
C(8)	−1660 (11)	10052 (8)	10020 (8)	35
O(9)	−85 (7)	8669 (4)	7837 (5)	25
C(10)	−808 (9)	8455 (6)	7257 (7)	19
C(11)	−1730 (9)	8213 (7)	7575 (9)	26
C(12)	−2471 (11)	8018 (7)	6984 (9)	27
C(13)	−2315 (12)	8050 (8)	6067 (9)	33
C(14)	−1366 (11)	8223 (8)	5761 (9)	30
C(15)	−591 (8)	8424 (6)	6321 (8)	21
C(16)	449 (9)	8581 (8)	5955 (7)	23
C(17)	749 (11)	9439 (7)	6094 (8)	30
C(18)	1174 (10)	7985 (7)	6367 (9)	26
C(19)	515 (11)	8416 (8)	4919 (9)	35
C(20)	8082 (10)	8109 (8)	8548 (10)	29
N(21)	793 (8)	10272 (6)	10502 (5)	25
C(22)	383 (12)	11071 (8)	10389 (10)	35
C(23)	1424 (10)	10251 (8)	11318 (9)	32
N(24)	2063 (8)	9037 (6)	9287 (6)	23
C(25)	2795 (11)	8739 (8)	9899 (9)	31
C(26)	2490 (11)	9094 (9)	8390 (9)	33
O(27)	2 (7)	8385 (4)	10265 (5)	21
C(28)	137 (9)	7639 (6)	10630 (7)	18
C(29)	564 (7)	7042 (6)	10106 (7)	18
C(30)	647 (10)	6272 (7)	10446 (9)	30
C(31)	383 (10)	6097 (8)	11295 (10)	34
C(32)	−45 (12)	6690 (7)	11828 (8)	31
C(33)	−199 (8)	7473 (7)	11505 (8)	24
C(34)	−731 (10)	8094 (7)	12095 (7)	27
C(35)	−1004 (12)	7770 (9)	13000 (9)	36
C(36)	−1670 (11)	8376 (9)	11611 (8)	30
C(37)	−51 (14)	8836 (8)	12243 (8)	33
C(38)	882 (11)	7230 (8)	9151 (9)	30

(10) Chisholm, M. H. *Polyhedron* **1983**, *2*, 681.
(11) Cotton, F. A.; Walton, R. A. "Multiple Bonds Between Metal Atoms"; Wiley: New York, 1982.
(12) Ahmed, K. J.; Chisholm, M. H.; Rothwell, I. P., Huffman, J. C. *J. Am. Chem. Soc.* **1982**, *104*, 6453.
(13) (a) Chisholm, M. H.; Cotton, F. A.; Frenz, B. A.; Reichert, W. W.; Shive, L. W.; Stults, B. R. *J. Am. Chem. Soc.* **1977**, *99*, 792. (b) Chisholm, M. H.; Cotton, F. A.; Extine, M.; Stults, B. R. *J. Am. Chem. Soc.* **1976**, *98*, 4477.

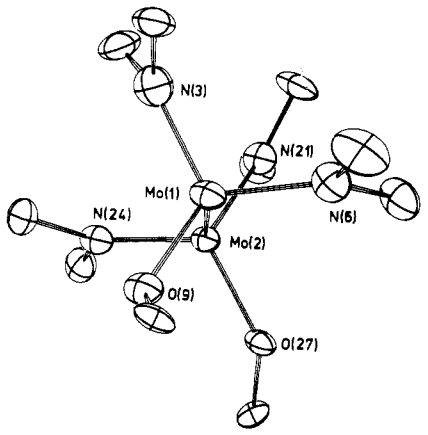

Figure 2. ORTEP view emphasizing the central skeleton of **1**. Two types of NMe_2 groups can be clearly seen: N(6), N(24) and N(3), N(21) due to the gauche rotamer that is adopted.

Table III. Selected Distances (Å) and Angles (deg) for Compound **1**

	Distances		
Mo(1)–Mo(2)	2.2198 (14)	Mo(2)–O(27)	1.971 (7)
Mo(1)–O(9)	2.003 (7)	Mo(2)–N(21)	1.961 (9)
Mo(1)–N(3)	1.936 (11)	Mo(2)–N(24)	1.925 (10)
Mo(1)–N(6)	1.957 (11)		
	Angles		
Mo(2)–Mo(1)–O(9)	103.2 (2)	Mo(1)–Mo(2)–Ni(21)	101.8 (3)
Mo(2)–Mo(1)–N(3)	102.4 (3)	Mo(1)–Mo(2)–N(24)	102.1 (3)
Mo(2)–Mo(1)–N(6)	102.5 (3)	O(27)–Mo(2)–N(21)	116.1 (3)
O(9)–Mo(1)–N(3)	117.5 (4)	O(27)–Mo(2)–N(24)	117.6 (4)
O(9)–Mo(1)–N(6)	117.4 (4)	N(21)–Mo(2)–N(24)	112.9 (4)
N(3)–Mo(1)–N(6)	110.9 (4)	Mo(1)–C(9)–C(10)	126.2 (7)
Mo(1)–Mo(2)–O(27)	103.3 (2)	Mo(2)–O(27)–C(28)	139.6 (8)

$Mo_2(NMe_2)_6$, even on extended heating in benzene solution.

Solid-State Structure of $Mo_2(OAr)_2(NMe_2)_4$ (1). An ORTEP view of **1** along with the numbering scheme used is given in Figure 1. Figure 2 shows a view looking along the metal–metal axis. Table I contains the crystallographic data while Tables II and III contain the fractional coordinates with the isotropic thermal parameter and some important bond distances and angles.

It can be seen that in the solid state the molecule adopts an "ethane-like" geometry about the di-metal center, typical of M_2X_6 compounds containing the $\sigma^2\pi^4$ electron configuration.[11] The unbridged $Mo_2O_2N_4$ central skeleton can be seen to adopt the gauche rather than the anti rotamer, with the aryloxides separated by a 45° torsion angle. The Mo–Mo distance of 2.22 Å is only slightly longer than that of $Mo_2(NMe_2)_6$[13a] and hence can be considered typical for the $(Mo{\equiv}Mo)^{6+}$ core. The conformation of the aryloxide ligands is worthy of note. It was expected that the use of the asymmetric OAr ligand would result in a conformation in which the plane of the aromatic ring would lie roughly parallel with the M–M axis, allowing the bulk *t*-Bu group to remove itself from the crowded di-metal center to a position roughly opposite the metal–metal bond. However, as can clearly be seen from Figure 2 the aryl plane is almost perpendicular to this axis. This conformation has been seen for a number of other 2,6-dialkylphenoxides coordinated to this particular di-metal center, and a possible electronic explanation has been proposed.[8] In order to try to relieve steric interactions both between ligands on the same metal and also across the metal–metal bond, the aryl groups are both bent away from the di-metal center to give Mo–O–Ar angles of 126 and 139°, considerably smaller than normally encountered for early-transition-metal phenoxides.[14] Despite this bending away of the aryl rings, the considerable bulk of the alkyl substituents is still felt by the two dialkylamido coligands. This can be seen by considering the coordination about each metal center individually. All three donor atoms are bent slightly away from a perfect trigonal-planar geometry with Mo–X (X = O or N) angles of 102 ± 1.5°. The Mo–OAr distances of 1.98 Å (average) are consistent with previous values for aryloxide ligands coordinated to such metal centers and are only slightly longer than the Mo–NMe_2 distances of 1.94 Å (average). The steric bulk of the OAr ligand has the effect of compressing together the two amido ligands, N–Mo–N = 112.5° (average) compared to O–Mo–N = 117.4° (average). It is interesting to compare these values with those found for the molecule $Mo_2R_2(NMe_2)_4$ (R = 6-methyl-2-methylpyridyl), a compound of related general formula $Mo_2X_2(NMe_2)_4$ that crystallizes in the gauche from (vide infra) but with a sterically very undemanding X substituent.[15] Here, the N–Mo–N angles are opened up to 121.5° (average) compared to N–Mo–C angles of 112.0° (average).

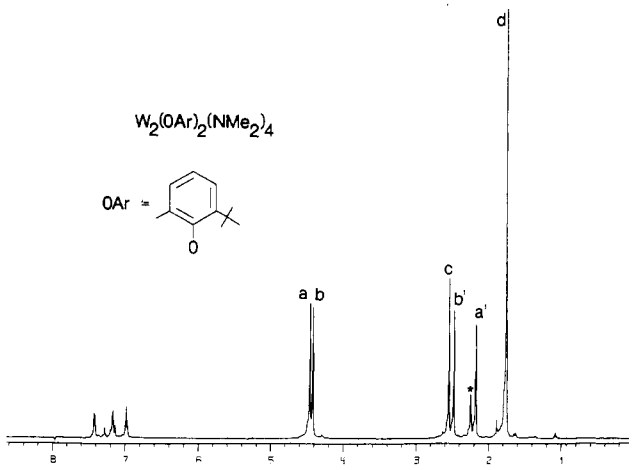

Figure 3. ^1H NMR spectrum (470 MHz; −20 °C/toluene-d_8) of $W_2(OAr)_2(NMe_2)_4$ (**2**). The four types of N-CH_3 resonances are indicated by a, a', b, and b'. The OAr-CH_3 group is labeled (c) with the OAr-*t*-*Bu* labeled (d).

Solution Structure and Fluxionality of 1 and 2. One interesting structural aspect of the chemistry of unbridged 1,2-$M_2X_2Y_4$ (M = Mo, W) type compounds is the possible existence of anti and gauche rotamers.[11] Structural studies have shown that both are possible in the solid state depending on substituents, and solution studies have shown that both may be present in equilibrium in solution.[11] Measurements of the rate of interconversion of such rotamers has allowed the energy for rotation about metal–metal triple bonds to be estimated.[16] The low-temperature (−20 °C) ^1H NMR spectra of both **1** and **2** are consistent with the presence in solution of the gauche rotamer. No signals identifiable with the anti rotamer could be seen. The spectrum of **2** at −20 °C (470 MHz) is shown in Figure 3. Both the qualitative appearance and temperature dependence of this spectrum is identical with the behavior found for solutions of **1**. The solid-state structure of the gauche rotamer (Figure 2) shows that there are two types of NMe_2 groups present, those close to the OAr group, N(6) and N(24), and those away, N(3) and N(21). Furthermore, the orientation of the NMe_2 groups lying parallel with the M–M axis results in each NMe_2 ligand having two types of CH_3 groups. Those lying over the metal–metal band are referred to as proximal and those away as distal. Hence, one predicts the presence in the ^1H NMR of four types of N–CH_3 resonances, and these are indicated (Figure 3). Those to lower field can be assigned as the proximal methyl groups, the anisotropy of the metal–metal bond causing them to be deshielded.[13] The other resonances in the spectrum can be assigned to the OAr ligand. The presence of four, sharp, well-resolved signals for the N–CH_3 groups leads to the following conclusions. First, rotation about the M–NMe_2 axis is slow on the NMR time scale due to the lack of exchange of proximal and distal methyl groups. Second, rotation about the

(14) Malhotra, K. C.; Martin, R. L. *J. Organomet. Chem.* **1982**, *239*, 159.

(15) Chisholm, M. H.; Folting, K.; Huffman, J. C.; Rothwell, I. P. *Inorg. Chem.* **1981**, *20*, 1496.

(16) Chisholm, M. H.; Huffman, J. C.; Rothwell, I. P. *Organometallics* **1982**, *1*, 251.

metal–metal bond is also slow as exchange between the two types of amido groups a and b does not occur at this temperature. Restricted rotation about both the M—N and M≡M bonds is a common feature of such systems.

Attempts to assign the two types of NMe_2 groups with the observed resonances have to be based on the temperature dependence of the NMR spectra. On warming up to room temperature, exchange of proximal and distal methyl groups occurs, but at different rates. Initially the proximal and distal resonances for one NMe_2 (b) begin to broaden and soon collapse into the base line while those for the other (a) remain relatively sharp. At higher temperatures the signals due to (a) broaden and also collapse. From the coalescence temperatures we can estimate the M–N rotational barriers (±0.5 K cal mol^{-1}, Mo in parentheses): (a) 17.1 (16.4); (b) 14.6 (13.3). This rotational barrier has both an electronic and steric component. The electronic part is due to the presence of considerable nitrogen p to metal d π bonding between the filled amido p orbital and the empty d_{xy}, $d_{x^2-y^2}$ orbitals on the molybdenum atom (assuming the M–M bond contains the z axis).[11] The unavailabilty of empty orbitals of correct symmetry means that this partial double bond is broken when the NMe_2 group rotates perpendicular to the M–M axis in order to exchange proximal and distal methyl groups. The steric contribution comes about from the size of the neighboring coligands also restricting the rotation ofthe NMe_2 plane perpendicular to the M–M axis. The difference in energy for rotation about these two sets of ligands is almost certainly steric. It is not easy to assess the steric environment for rotation about the two types of M–NMe_2 bonds (Figures 1 and 2). The two types of NMe_2 groups are those that can be considered anti to the OAr groups, N(3) and N(21), and those gauche, N(6) and N(24). These two types of groups can be seen to have different steric environments due to interactions across the metal–metal bond. However, due to the asymmetry of the OAr ligand they are also nonequivalent due to the fact that one set is close to the *t*-Bu group of the aryloxide while the other set is close to the Me group. The set of amido ligands, N(6) and N(24), do appear to have the most sterically crowded environment, but no definitive assignment is possible with the available data.

One would predict that on raising the temperature eventually the proximal and distal methyl groups would collapse to give a limiting spectrum containing two singlets due to the two types of NMe_2 groups. However, this assumes that rotation about the M–M bond is not facile on the NMR time scale at this temperature or else exchange of amido environments would occur, leading to only a single resonance at high temperature. Unfortunately, high-temperature limiting spectra could not achieved (vide infra; maximum temperature was 115 °C/90MHz), and hence it cannot be concluded if metal–metal bond rotation is facile in these systems. It is interesting to note that exchange of the two amido environments requires not only rotation about the metal–metal bond but also a rotation of the OAr ligand plane. This is due to the asymmetry of the aryloxide ligand. In the crystal chosen, all of the molecules were of one enantiomeric type. The act of exchange of amido environments hence involves exchange between the two types of gauche enantiomers.

Thermal Stability of Compounds. Despite the apparently unfavorable orientation of the aryl rings in the structure of **1** for metalation of the ligand across the metal–metal bond, the complexes were subjected to extended thermolysis. On heating at 125 °C for periods of hours in toluene-d_8, both complexes undergo decomposition. The ^1H NMR spectrum of the resulting solutions shows copious amounts of dimethylamine along with a multitude of signals between δ 1.5 and 5.0. We have been unable to either spectroscopically identify or physically isolate any metal-containing product from these solutions. Thermolysis in the presence of pyridine also results in the formation of similar solutions. The cause of this thermal instability in contrast to the compounds $M_2(NMe_2)_6$ and $M_2(OAr')_4(NMe_2)_2$ (OAr′ = 2,6-dimethylphenoxide) may indeed be due to the cyclometalation of the alkyl side chains to generate a dimethylamine leaving group. However, it is also possible that the overall steric bulk in the molecule results in other reactions or decomposition pathways involving the metal–metal bond or dimethylamido coligands.

Experimental Section

Preparation of 1,2-$M_2(OAr)_2(NMe_2)_4$ [M = Mo (1), W (2)]. To a solution of $Mo_2(NMe_2)_6$ (0.50 g, 1.10 mmol) in hexane (25 mL) was added 2-*tert*-butyl-6-methylphenol (HOAr, 0.42 g, 2.52 mmol), and the mixture was allowed to stir at 25 °C for 4 h. Removal of solvent under vacuum followed by addition of hexane (20 mL) and cooling to −15 °C gave yellow crystals of products in good yield. Anal. Calcd for $Mo_2C_{30}H_{54}N_4O_2$: C, 51.87; H, 8.06; N, 7.84. Found: C, 51.98; H, 8.10; N, 7.83. ^1H NMR (−20 °C, C_7D_8): δ 6.90–7.40 (m, OC_6H_3Me-*t*-Bu), 4.45 (s, NMe_2^a), 2.16 (s, $NMe_2^{a'}$), 4.22 (s, NMe_2^b), 2.60 (s, $NMe_2^{b'}$), 2.41 (s, OC_6H_3*Me*-*t*-Bu), 1.69 (s, OC_6H_3Me-*t*-*Bu*). Use of $W_2(NMe_2)_6$ gave **2** under identical conditions. Anal. Calcd for $W_2C_{30}H_{54}N_4O_2$: C, 41.32; H, 6.42; N, 6.24. Found: C, 41.58; H, 6.28; N, 6.21. ^1H NMR (−20 °C, C_7D_8): δ 6.90–7.40 (m, $OC_6H_3M_2$-*t*-Bu), 4.40 (s, NMe_2^a), 2.05 (s, $NMe_2^{a'}$), 4.35 ns, NMe_2^b), 2.35 (s, $NMe_3^{b'}$), 2.50 (s, OC_6H_3*Me*-*t*-Bu), 1.70 (s, OC_6H_3Me-*t*-*Bu*).

X-ray Structure Determination for 1,2-$Mo_2(OAr)_2(NMe_2)_4$ (1). General procedures have been described previously.[17] The well-formed, pale yellow crystal chosen for the study was mounted on a glass fiber with silicon grease. After transfer to the geniostat and cooling to −160 °C, a systematic search of a limited hemisphere of reciprocal space revealed an orthorhombic lattice with only axial extinctions, indicating the noncentric space group $P2_12_12_1$, a choice later confirmed by statistical tests and the solution and refinement of the structure.

The structure was solved by a combination of direct methods (MULTAN78) and Fourier techniques. All hydrogen atoms were located and refined. The final refinement included all positional parameters and thermal parameters (anisotropic for Mo, N, O, and C; isotropic for H), as well as an overall scale factor and isotropic extinction parameters. ψ scans of several reflections located near θ = 90° were flat, indicating no absorption correction was necessary.

The coordinates listed are for the proper enantiomorph for the crystal studied, based on identical refinements with both enantimers.

A final difference Fourier was featureless, the largest peak being 0.21 eÅ^3.

Acknowledgment. We thank the National Science Foundation (Grant CHE-8219206 to I.P.R.) for support of this work. T.W.C. gratefully acknowledges receipt of a David Ross Fellowship from the Purdue Research Foundation. We thank Purdue University Biochemical Magnetic Resonance Laboratory supported by NIH Grant RR01077 from the Biotechnology Resource Program of the Division of Research Resources. We also thank G. Niccolai for technical assistance.

Supplementary Material Available: Listings of fractional coordinates and isotropic thermal parameters, anisotropic thermal parameters, complete bond distances and angles, and observed and calculated structure factors (25 pages). Ordering information is given on any current masthead page.

(17) Huffman, J. C.; Lewis, L. N.; Caulton, K. G. *Inorg. Chem.* **1980**, *19*, 2755.